2026 IEEE International Conference on Robotics and Automation (ICRA 2026)
June 1-5, 2026. Vienna, Austria

FRESHR-GSI: A Generalized Safety Model and Evaluation Framework for Mobile Robots in Multi-Human Environments

Pranav Pandey Ramviyas Parasuraman Prashant Doshi

***Abstract*— Human safety is critical in applications involving close human-robot interactions (HRI) and is a key aspect of physical compatibility between humans and robots. While measures of human safety in HRI exist, these mainly target industrial settings involving robotic manipulators. Less attention has been paid to settings where mobile robots and humans share the space. This paper introduces a new robot-centered directional framework of human safety. It is particularly useful for evaluating mobile robots as they operate in environments populated by multiple humans. The framework integrates several key metrics, such as each human's relative distance, speed, and orientation. The core novelty lies in the framework's flexibility to accommodate different application requirements while allowing for both the robot-centered and external observer points of view. We instantiate the framework by using RGB-D based vision integrated with a deep learning based human detection pipeline, termed FRESHR (Framework for RGB-D based Evaluation of Safety of Humans for mobile Robots), to yield a proxemics-guided generalized safety index (GSI) that instantaneously assesses human safety. We extensively validate GSI's capability of producing appropriate and fine-grained safety measures in real-world experimental scenarios and demonstrate its superior efficacy against extant safety models.**

I. Introduction

The study of human-robot interaction (HRI) and collaboration has gained importance as more humans and robots share workspaces and engage in proximal encounters [1]. Robot co-workers can significantly enhance productivity and efficiency in repeatable and collaborative tasks. For this, the interacting human and robot must be physically compatible, and a key aspect of such compatibility is human safety [2].

A substantial body of literature focuses on human safety in industrial settings [3], with established safety criteria and guidelines for collaborative robots [4], [5] including industrial robot safety standards such as ISO 10218 and ISO/TS 15066 [3], [6]. Researchers have also introduced real-time safety assessments for large manipulators in human-robot collaborations [7], [8], [4]. While appropriate for close proximity and contact interactions, such as in manufacturing, these safety standards and measures cannot be readily transferred to mobile robots, which typically operate in large, unbounded workspaces, where the mobility of humans and robots significantly impacts human safety. Furthermore, existing methods in the literature tend to underestimate safety in multi-human environments. As such, there is a need for scalable measures of safety that can be obtained from different points of view (proprioceptive/exteroceptive) and for different utilities, such as safety assessments and motion control.

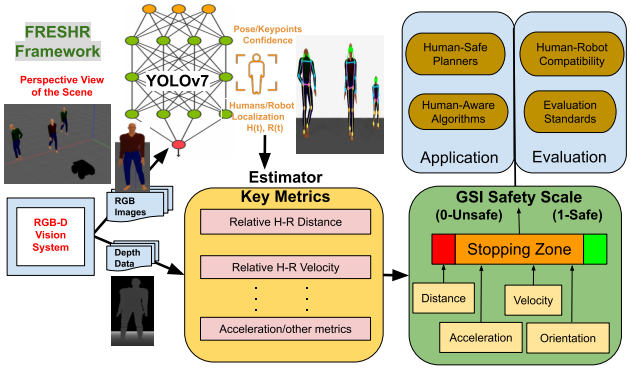

Fig. 1: Overview of the proposed vision-based safety evaluation framework (FRESHR). A continuous sequence of RGB images is supplied to Yolov7 for human and robot detection and pose estimation. These detections and their confidence values is integrated with depth information to compute key metrics such as the relative distance and velocity. Finally, a proxemics-guided Generalized Safety Index (GSI) is derived to evaluate the multi-human safety.

In this paper, we introduce FRESHR (Framework for RGB-D based Evaluation of Safety of Humans for mobile Robots), a framework for evaluating the physical safety of multiple humans in shared human robot workspaces. The framework integrates multi-modal data from depth cameras mounted on the robot or an external observer to assess human safety. We derive the *Generalized Safety Index (GSI)* for mobile robots by combining distance, relative velocity, and bearing between the robot and nearby humans.

FRESHR sets itself apart from other vision-based measurement systems by enabling safety evaluation from multiple points of view: from the robot, supporting human-aware control, from an external observer of the HRI, or another robot in a multi-robot system, assessing the safety of humans interacting with other robots. Moreover, GSI is a proxemics-guided fine-grained safety assessment model, bounded between 0 and 1, where 0 represents an unsafe condition and 1 indicates full safety. Unlike existing safety scales that primarily focus on short-distance collaborations between a *single* human and a manipulator, GSI extends to multi-human HRI settings by prioritizing the safety of those at greater risk than averaging across multiple humans. Notably, GSI is designed solely for safety evaluation rather than active robot control, ensuring an accurate assessment of human safety without dictating motion responses. Together, FRESHR-GSI is suitable for use in large, crowded environments, making it a versatile tool for safety analysis. Demonstrations in real-world environments are provided in the attached video. These contributions are

Research was sponsored by the DEVCOM Analysis Center and was accomplished under Cooperative Agreement Number W911NF-22-2-0001.
The authors are with the School of Computing, University of Georgia, Athens, USA. Emails: {pranav.pandey,ramviyas,pdoshi}@uga.edu

pivotal to motivating and stimulating further innovations in the evaluation and improvement of human safety around mobile robots.

II. Related Work

Proxemics [9] studies how people manage distance during interaction. Hall defined four zones: intimate (0–0.46m), personal (0.46–1.2m), social (1.2–3.7m), and public (>3.7m), widely used in HRI [10], [11]. Human subject studies [12], [13] report safer interactions when robots stop in the personal zone and discomfort when they enter the intimate zone. A safety measure should therefore give graded values, high beyond the public zone and low when the intimate zone is breached. Building on this proxemics motivation, Spurny et al. [14] introduce a golden-ratio (GR) based dynamic proxemics model that adaptively partitions comfort zones.

Many HRI metrics evaluate safety and performance [15], but fewer target mobile robots in dynamic shared spaces [16]. Vision based speed and separation monitoring is easier to deploy than fixed industrial safety zones [17]. Prior work uses deep learning for collision detection [18] and combines tracking with zones derived from human speed and robot reaction time [19]. RGB-D sensing can improve detection and tracking, including keypoints for speed and separation with force limiting [20], top view RGB-D for operator localization [21], and skeletal tracking as an alternative to wearables [22]. However, these methods are mostly evaluated from fixed exteroceptive viewpoints and do not provide a proprioceptive safety assessment for mobile robots.

Several safety fields and indices from planning and control were developed mainly for single human settings. Kulic and Croft [7] proposed a Danger Index (DI) using distance and velocity, Lacevic et al. [23] introduced the Kinetostatic Danger Field (KDF), Lippi et al. [8] extended KDF into a Human Safety Assessment (HSA), and Palmieri et al. [4] proposed the Human Safety Field (HSF). These scales are typically unbounded and require design cutoffs. Multi human use is often suggested by averaging (for example in HSF [4]), but it is not explicitly validated in dynamic multi human settings. Other formulations combine distance, velocity, orientation, and inertia through sums or products, which can misestimate safety. In particular, averaging across humans can hide risk to a nearby person when others remain far away.

To address these gaps, we propose a bounded multi human safety model grounded in proxemics, mapping observable factors (distance, velocity, orientation) into robot stopping zones with strict bounds. GSI uses exponential terms to reflect non linear trends in subjective safety perception and to support task level customization, consistent with human centered framing of physical safety in HRI [24]. Moreover, recent works have explored certifiable safety and control guarantees for mobile robots. By contrast, GSI serves as a real time safety assessment metric, allowing for future integration with a safety controller.

III. FRESHR: Evaluating Human Safety

Let a mobile robot r with pose, $p_r = \langle \boldsymbol{x}_r, \theta_r \rangle$ where $\boldsymbol{x}_r = (x_r, y_r, z_r)$, be positioned in conjunction with multiple humans, $\{h_i | i = 1 \dots N_h\}$ where N_h is the number of detected humans. Let a human h_i be detected at a position $\boldsymbol{x}_{h_i} = (x_i, y_i, z_i)$ in a common frame of reference. The frame may be centered on the robot or global based on an external observer. We assume that the robot's motion constraints (e.g., maximum speed V_{max} and maximum deceleration A_{max}) are known, the robot has an RGB-D vision system to estimate the relative distance and velocities between every detected human and the robot (see Sect. III-B), and the robot runs algorithms to detect and localize multiple humans [25] within the sensor's field of view. The problem facing FRESHR is to determine the current level of physical safety of all detected humans h_i around the robot r in its direction of travel θ_r.

A. Generalized Safety Index

In our framework, three key components are integrated to assess the safety of every detected human: distance, relative velocity, and the bearing of the human from the robot. These measures are generally deemed sufficient for assessing safety within the interaction space [5].

For each human h_i at position $\boldsymbol{x}_{h_i}$ in a common reference frame, let $d_{h_i,r}$ denote the distance from the robot, $d_{h_i,r} = \|\boldsymbol{x}_{h_i} - \boldsymbol{x}_r\|_2$. The relative velocity between them is the first-order derivative of the distance, $v_{h_i,r} = -\dot{d}_{h_i,r}$, which is a positive value when the distance between human and robot decreases and a negative value otherwise. Denote the relative bearing of the human h_i w.r.t. the robot as $\theta_{h_i,r} = \measuredangle(\boldsymbol{x}_{h_i} - \boldsymbol{x}_r) - \theta_r$. To clarify, this bearing is the angle (measured counterclockwise from the positive x-axis) between the segment joining the robot to the human and the robot's current orientation θ_r.

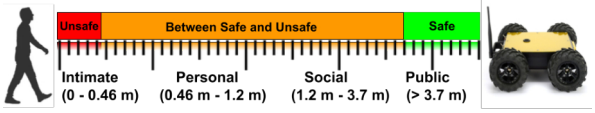

Fig. 2: FRESHR aligns its safety scale with the well-established proxemics ranges in HRI spaces. GSI takes a value of 1, indicating safe (green) in the public space, (0 - 1] (amber) in the personal and social spaces, and 0 (red) in the intimate space.

To arrive at a proxemics-guided safety scale, we rely on the well-known concepts of intimate, personal, social, and public spaces of human-robot interactions [9], which are illustrated in Fig. 2. Generally, a human's intimate space was empirically determined to be a sphere of radius 0.46m centered on the human, her personal and social spaces are the spherical shells whose radius lies in (0.46m - 1.2m] and (1.2-3.7m] ranges respectively, and the region beyond 3.7m is considered a public space. Our approach is to assess human safety based on where and whether the mobile robot intrudes into these spaces (i.e., the stopping zone). Towards this, we define a generalized safety index of a human h_i as

$$\widehat{GSI}_{h_i}(d_{h_i,r}, v_{h_i,r}; \rho) = \left[\frac{d_{h_i,r} - \left(\mathrm{s}(v_{h_i,r}) \frac{v_{h_i,r}^2}{2A_{max}} + D_{min} \right)}{D_{max} - D_{min}} \right]^{\rho} \tag{1}$$

Here, A_{max} is a constant representing the maximum (de-)acceleration of the robotic platform; D_{max} is the distance

beyond which the human's safety is assured – we may let $D_{max} = 3.7m$ (public space), and a mobile robot should not come closer than D_{min} – we may let $D_{min} = 0.46m$ (intimate space), or 0 if, for example, the robot needs to transport the human. The term $\frac{v_{h_i,r}^2}{2A_{max}}$ in (1) indicates the distance required for the robot to stop at its current relative speed $v_{h_i,r}$, given a maximum deceleration rate of A_{max}. $s(v_{h_i,r})$ is the sign function that informs whether the human is approaching or moving away from the robot. The sign function is positive when the distance between the human and the robot decreases over time and negative otherwise.

The hyperparameter $\rho > 0$ provides a way to fit GSI to various kernels based on the current application setting and the subjective human perception of safety. We may select different values of ρ in applications involving GSI-aided motion control, where higher $\rho > 1$ decay of safety can be appropriate in robots with slow reaction times or large mass (i.e., a larger than usual buffer from the human is preferred for more cautious human perceptions of safety or higher chances of a platform failure to stop in fast motion settings [26]. Previous work has utilized a similar parameter for industrial robots, where it is set to 2 [7]. On the other hand, lower values of $\rho < 1$ may be utilized if the human is comfortable around mobile robots [27], reducing the need for unnecessary interventions [7]. Finally, a balanced trend can be obtained with $\rho = 1$ providing a rational GSI [26], and therefore, we use this setting ($\rho = 1$) for assessing the current safety level. Fig. 3 illustrates the impact of ρ on the GSI model.

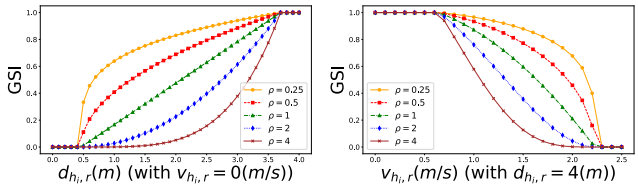

Fig. 3: GSI can be fitted to various applications, robot platform properties, and subjective safety perceptions of humans through parameter $\rho > 0$. For instance, $\rho = 1$ is set for assessing safety, $\rho > 1$ for more cautious robot control, and $\rho < 1$ for a more closer interaction with human who are already comfortable.

In essence, $\widehat{GSI}_{h_i}$ accounts for the robot's ability to stop before breaching the intimate zone of a human and we bound it between 0 and 1, so any value less than 0 will be set to 0 and any value greater than 1 is set to 1. A value $= 0$ represents an unsafe condition (i.e., the intimate space has or is about to be breached), while GSI $= 1$ asserts a fully safe condition (i.e., the robot is in the public zone). Any value between 0 and 1 measures the safety level, closer to 0 indicates less safety, and higher risk to the human at that point in time, whereas closer to 1 suggests that the human is likely to be safe at that time.

Eq. 1 is applicable for a static scenario or if we assume the robot and human are directly approaching each other, i.e. $\theta_{h_i,r} = 0^\circ$. For a non-zero bearing of the human w.r.t. the robot, we extend Eq. 1 to scale the GSI with how close the robot gets to the human as it passes by it. More specifically, we obtain a directional GSI in FRESHR as given below,

$$GSI_{h_i}(d_{h_i,r}, v_{h_i,r}, \theta_{h_i,r}; \rho) = 1 - (1 - \widehat{GSI}_{h_i}) \cos\theta_{h_i,r}. \tag{2}$$

We illustrate the derivation of Eq. 2 using Fig. 4(a), which shows that $\cos\theta_{h_i,r}$ can be used to scale the complement of the GSI value that is obtained as if the robot is heading straight for the human. The $\cos\theta$ dependence reflects that humans tolerate side and rear approaches more than head-on approaches, consistent with prior HRI user studies on approach comfort [28]. Notice that when $\theta_{h_i,r} = 0$, $\cos\theta_{h_i,r} = 1$ and $GSI_{h_i}(d_{h_i,r}, v_{h_i,r}, \theta_{h_i,r}; \rho)$ collapses to $\widehat{GSI}_{h_i}(d_{h_i,r}, v_{h_i,r}; \rho)$ as we may expect. And, if $\widehat{GSI}_{h_i}(\cdot)$ indicates not safe, then $GSI_h(\cdot)$ tempers down the non-safety by how close the robot is expected to pass by the human. Thus, GSI represents a dynamic measure of safety, integrating real-time motion input to assess the human's safety in the shared workspace, given the robot's movement.

Remapping GSI to Proxemic Zones: We can map the normalized GSI $\in [0, 1]$ to an equivalent stopping distance

$$d_{\text{stop}} = D_{\min} + (D_{\max} - D_{\min})\,\text{GSI}^{\,1/\rho}, \tag{3}$$

where $D_{\min} = 0.46\,\text{m}$ and $D_{\max} = 3.70\,\text{m}$ are Hall's intimate and public thresholds, and $\rho > 0$ is the same shaping parameter used in Eq. 1. We then compare d_{stop} to anisotropically scaled proxemic boundaries

$$B_i(\theta) = B_i\,[1 + \beta\cos\theta], \quad \beta \in [0, 1), \tag{4}$$

so that frontal approaches ($\theta = 0$) expands the comfortable distance than side approaches. Zone assignment follows $d_{\text{stop}} \in [B_i(\theta), B_{i+1}(\theta))$ for $i \in \{\text{intimate}, \text{personal}, \text{social}, \text{public}\}$. When needed, we can further split each zone interval using the golden ratio $\varphi = 1.618$ [14].

GSI for settings shared with multiple humans Implications of robot motion on the safety of multiple humans (e.g., in crowded pedestrian areas [29]) are studied from motion planning and physiological social awareness perspectives [16], [30]. The presence of multiple humans in the shared workspace complicates the determination of safety as we now face an additional challenge: how to aggregate individual safety indications to determine the safety of the whole.

Previous work (HSF [4]) advocates averaging individual safety values in all humans. But, the disadvantage with it is it may *overestimate* the overall safety when the robot is safe for a majority of the humans in the group but unsafe for a few in the shared space. Therefore, we posit that the safety index for the whole should not only be directional but should also attribute higher importance to the safety of those humans for whom the robot presents significant safety implications in its intended direction. Toward this, let $\boldsymbol{d}_{h,r} = \langle d_{h_i,r} | i = 1, \ldots, N_h \rangle$ represent the vector of relative distances between the mobile robot and each human i in the shared space and analogously $\boldsymbol{v}_{h,r}$ and $\boldsymbol{\theta}_{h,r}$ represent the vector of relative velocities and angles, respectively. Rather than simply returning the minimum of the $GSI_h(\cdot)$ values, we utilize a smooth minimum LogSumExp (also known as the

realsoftmin) of the individual values, to obtain the *collective GSI* for the group of N_h humans in the robot's shared space.

$$GSI(\boldsymbol{d}_{h,r}, \boldsymbol{v}_{h,r}; \boldsymbol{\theta}_{h,r}; \rho, \tau) = \\ -\tau \ln \left(\frac{1}{N_h} \sum_{i=1}^{N_h} e^{\frac{-GSI_{h_i}(d_{h_i,r}, v_{h_i,r}, \theta_{h_i,r}; \rho)}{\tau}} \right) \quad (5)$$

where $GSI_h(\cdot)$ is as defined previously in Eq. 2 for a single human in the vicinity, τ is a hyperparameter that controls the smoothness of the approximation of the minimum of the $GSI_h(\cdot)$ values. As τ reduces, GSI converges to the minimum $GSI_h(\cdot)$ across all humans i (see Fig 4(b)). We set $\tau = 0.01$ for obtaining close to the absolute minimum. The LogSumExp function heavily penalizes larger $GSI_h(\cdot)$, which makes it sensitive to the small $GSI_h(\cdot)$ values, thereby obtaining a safety index corresponding to the human that influences the most. GSI in Eq. 5 satisfies the core properties of safety measures [8], [23] such as a monotonic increase (decrease) with distance (velocity) and differentiability. These properties enable a differential safety scale that is useful in evaluating and integrating mobile robot algorithms. For instance, similar to [23], GSI can be vectorized for control applications as

$$\overrightarrow{GSI}(t) = GSI(\boldsymbol{d}_{h,r}, \boldsymbol{v}_{h,r}; \boldsymbol{\theta}_{h,r}, t; \rho). \frac{\nabla GSI(t)}{\|\nabla GSI(t)\|}, \quad (6)$$

where ∇ is either the time-based or pose-based derivative. Finally, if the collective also includes multiple mobile robots, FRESHR can further generalize to obtain the GSI per human that is a smooth minimum across the collective GSIs w.r.t. all the robots. We summarize GSI for various scenarios in Table I and compare it with other scales for appropriateness.

B. FRESHR Implementation

We develop a real-time RGB-D-based system to measure robot safety during interactive tasks and integrate this with our GSI scale (see Fig. 1). We chose vision-based because it is widely available in mobile robots; however, the core GSI calculations remain valid even if human detection or tracking is replaced by another sensor system. The use of depth point clouds to obtain the relative distance between the robot and humans allows flexibility in the deployment from different viewpoints, such as external agents or sensors on board the robot, ensuring safety and comfort for humans. At its core, the framework employs a deep learning pipeline for detecting humans and robots, and uses algebraic calculations on RGB-D measurements to extract safety related factors such as distance, relative velocity, and bearing.

We applied YOLO-v7 [25] for real-time human detection/localization from RGB images, providing skeleton keypoint locations for whole-body safety. These detections are correlated with depth data from synchronized images. YOLO provides confidence scores for each detection, useful for integrating multiple detections. Detected pixel locations are converted to world frame coordinates using the OpenCV library, applying the camera's intrinsic matrix. This is integrated with depth information to estimate real-world 3D coordinates

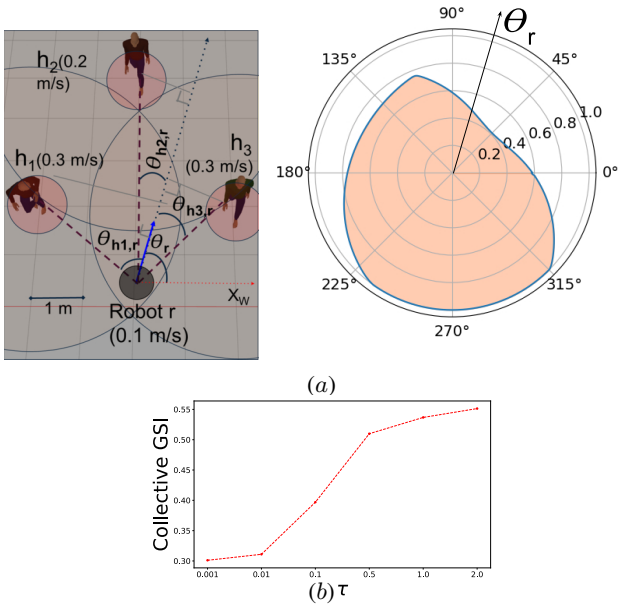

Fig. 4: (a) An example setting with three humans in the vicinity of the mobile robot r. FRESHR yields a directional safety value for each human. In this example, $GSI_{h_1} = 0.7$ with $\theta_{h_1,r} = 290^\circ$, $GSI_{h_2} = 0.9$ with $\theta_{h_2,r} = 345^\circ$, and $GSI_{h_3} = 0.3$ with $\theta_{h_3,r} = 30^\circ$, each of which is calculated using Eq. 2. (b) Impact of the hyperparameter τ on the collective GSI (polar plot in (a)) obtained using Eq. 5. The individual GSIs used are those from (a).

for each object (human position p_h, robot position p_r, and relative orientation $\theta_{h_i,r}$). For each human, the keypoints are combined by weighted addition $d_{hr} = \sum_k w_k d_k$, with confidence scores as weights w_k for the k^{th} keypoint at a relative distance of $d_k = \|p_r - k\|$. Scores are normalized such that $\sum_k w_k = 1$. Keypoints passing a confidence threshold $conf_{thr}$ allow us to remove noisy detections. We set $conf_{thr} = 0.9$ for the best detection accuracy.

The camera frame acts as the global reference frame, and $\boldsymbol{d}_{h,r}, \boldsymbol{v}_{h,r}; \boldsymbol{\theta}_{h,r}$ in the robot's frame can be obtained using the camera's rotation and translation matrices if the camera is rigidly mounted on the robot. Euclidean norm is used for distances. For geometric rigidity, we use three distance measurements for robust velocity estimates, i.e., $v_{hr} = \sqrt{\frac{d_{hr}^2(t-2) - 2d_{hr}^2(t-1) + d_{hr}^2(t)}{2}}/(T)$, where $\frac{1}{T}$ is the measurement frequency. If no detections are made (e.g., low detection confidences, out of sensor range, or due to occlusions), the estimates will not be used at that time.

IV. Experimental Evaluation

We conducted extensive experiments and validate FRESHR by (i) verifying distance, velocity, and bearing estimates in simulation, (ii) comparing GSI with existing safety scales in two real-world multi-human robot experiments, and (iii) analyzing crowd–robot datasets to demonstrate its usefulness in analyzing human-aware motion planning.

A. Validating FRESHR Measurements

As the accuracy of GSI is contingent on correctly measuring the human's distance and relative velocity, we begin by

TABLE I: A summarization of the appropriateness of different safety scales in various scenarios (combinations of distance $d_{h_i,r}$ and relative velocity $v_{h_i,r}$). The appropriate safety level is determined based on the stopping zone of the robot to the closest human (Fig. 2). SH - single human. MH - multi-human. A ✓or × indicates whether the scale may correctly inform the appropriate safety level per the proxemics framework. ↑ and ↓ denote the possibility of overestimating or underestimating the safety levels, respectively.

Scenario	Distance	Relative Velocity	Stopping Zone	Appropriate Assessment	**GSI** [Ours]		**DI** [7]		**KDF** [23]		**HSF** [4]		**HSA** [8]		**GR** [14]	
					SH	MH	SH	MH	SH	MH	SH	MH	SH	MH	SH	MH
A	$d_{h_i,r} \geqslant D_{max}$	$v_{h_i,r} \leqslant 0$	Public	Safe	✓	✓	✓	N/A	✓	✓	✓	✓	✓	✓	✓	N/A
B	$d_{h_i,r} \geqslant (D_{max} + \frac{v_{h_i,r}^2}{2A_{max}})$	$v_{h_i,r} \geqslant 0$	Public	Safe	✓	✓	✓	N/A	✓	✓	✓	✓	✓	✓	✓	N/A
C	$d_{h_i,r} \geqslant D_{max}$	$0 < v_{h_i,r}^2 < 2A_{max}(d_{h_i,r} - D_{min})$	Within Personal/Social	Between	✓	✓	× ↑	N/A	✓	✓	× ↑	× ↑	✓	✓	✓	N/A
D	$D_{min} \leqslant d_{h_i,r} \leqslant D_{max}$	$v_{h_i,r} = 0$	Within Personal/Social	Between	✓	✓	× ↑	N/A	✓	× ↑	✓	✓	✓	✓	✓	N/A
E	$d_{h_i,r} \geqslant D_{max}$	$v_{h_i,r}^2 \geqslant 2A_{max}(d_{h_i,r} - D_{min})$	Intimate	Unsafe	✓	✓	× ↑	N/A	✓	× ↑	× ↑	× ↑	× ↑	× ↑	× ↑	N/A
F	$d_{h_i,r} \leqslant (D_{min} + \frac{v_{h_i,r}^2}{2A_{max}})$	$v_{h_i,r} \geqslant 0$	Intimate	Unsafe	✓	✓	✓	N/A	✓	✓	✓	✓	✓	✓	✓	N/A
G	$D_{min} \leqslant d_{h_i,r} \leqslant D_{max}$	$v_{h_i,r}^2 \leqslant -2A_{max}(D_{max} - d_{h_i,r})$	Public	Safe	✓	✓	✓	N/A	× ↓	× ↓	× ↓	× ↓	× ↓	× ↓	✓	N/A

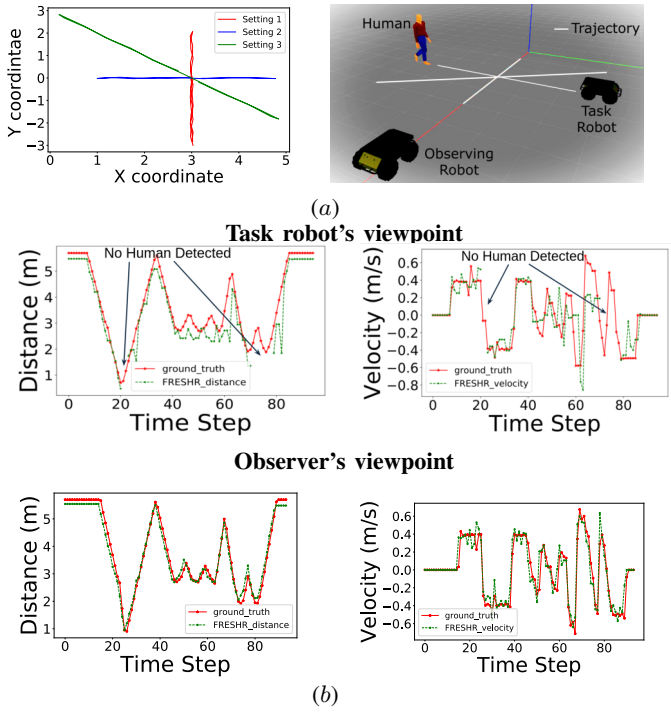

Fig. 5: (a) Human moves along three trajectories in the shared space: straight toward the task robot (setting 1), perpendicular to the task robot (setting 2), and diagonal (setting 3). (b) FRESHR-based estimation of the distances (left) and relative velocities (Right) from two different viewpoints.

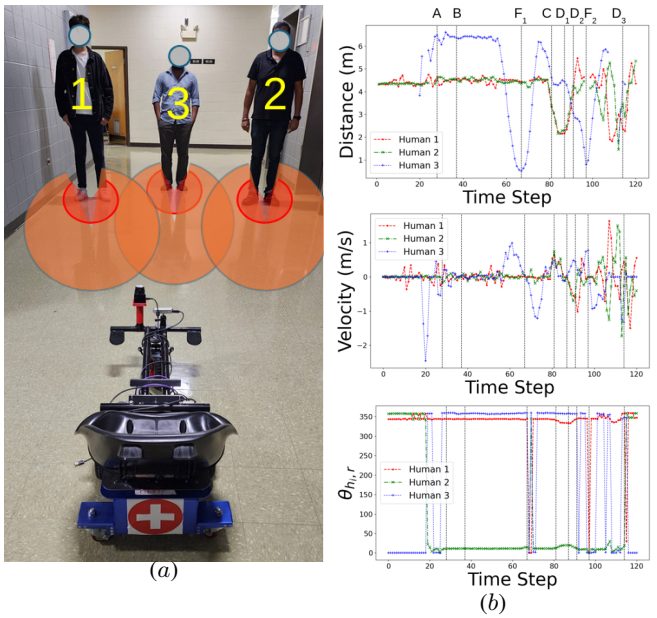

Fig. 6: (a) Setting for the physical robot experiment involving FRESHR on an Ubiquity Magni which is sharing space with three moving humans. (b) Validation of distances $\boldsymbol{d}_{h,r}$, relative velocities $\boldsymbol{v}_{h,r}$, and bearings $\boldsymbol{\theta}_{h,r}$ of the three humans.

assessing the error in obtaining these using typical sensors. We compare the FRESHR-provided distance and relative velocity with ground truth for a single human as she follows the trajectories shown in Fig. 5(a) in ROS Gazebo 11. The perceived distance and velocity measurements are obtained using the RealSense camera D435i model provided by Intel and YOLO v7. Figure 5 shows that we can follow the change in distance in real time with reasonable accuracy. Although GSI can be computed at the full 30 Hz camera rate, we restrict it to 1 Hz to ensure stable updates and to avoid repeated zero-velocity estimates when human motion is slow. The mean absolute error in distance measurements are 11.3% and 5.07% from the task robot and the observer's viewpoints, respectively. Similarly, we observed the following error in the velocity measurements of the task robot at 16.6% compared to the observer robot's at 9.61%. These rates appear high because ground truth recorded zero velocity during "standstill" phases, whereas natural micro-movements were detected by the depth sensor, inflating the error. The D435i's specified accuracy is $\sim 2\%$ at 2 m, confirming that the sensing is within expected limits. Observer measurements were generally more accurate due to reduced occlusion. GSI requires these input metrics to be reliable for safety assessment. Importantly, we expect GSI from an observer's viewpoint to be much more accurate than from the task robot's viewpoint because an observer usually maintains a clear view of both the human and the task robot in its range and it often captures blind spots or occlusions present in the robot's onboard view. On the other hand, a moving human may not stay in the camera view of a navigating or stationary robot. In our setup, the observer and task robot do not share data. Since GSI is used only for evaluation, we do not implement fusion; a future multi-robot extension could use a publish–subscribe scheme to maximize coverage and reduce occlusion.

B. Validating Multi-Human Safety Assessment with GSI

Task robot's viewpoint: We conducted physical robot experiments with a Ubiquity Magni platform customized for use in a medical evacuation application [31] and equipped with an Intel RealSense D435i mounted in front, as we show in Fig. 6(a). We created a multi-human scenario with three humans in the robot's view simultaneously. While the robot

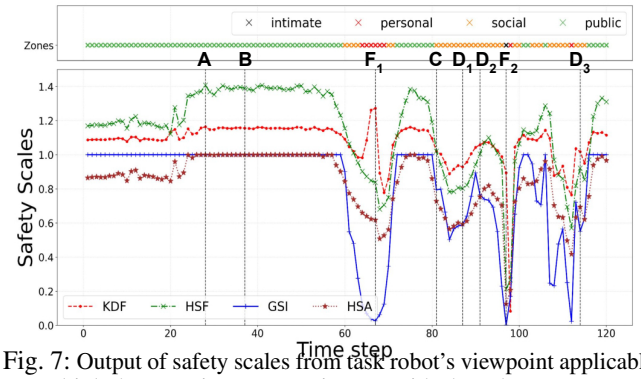

Fig. 7: Output of safety scales from task robot's viewpoint applicable to multiple humans in our experiments with three humans.

was stationary, the humans followed various trajectories at regular walking speeds to simulate a pedestrian walkway. This included: 1) Human 3 alone walks toward the robot and then moves away. Other humans stay put; 2) Humans 1 and 2 walk toward the robot while Human 3 stays put; 3) Human 3 walks toward the robot while Humans 1 and 2 walk away; and 4) Random movement of all humans. The attached video provides a detailed demonstration of the experiments.

We compare the GSI safety scale (with $\rho = 1$ for linear decay; $\rho > 1$ yields more conservative and $\rho < 1$ more permissive behavior) with the existing KDF [23], HSF [4], and HSA [8], considering the averaging approach for safety calculations in a multi-human environment per their designs. For comparison, we invert KDF since it is formulated as a danger field and normalize HSF by $D_{\max}$ to place all outputs on a common $[0, 1]$ scale for visualization. We note that KDF and HSF were originally designed for control oriented formulations rather than bounded evaluation scores, so this remapping is used only to enable consistent plotting and qualitative comparison across multi human scenarios. We show the distances, velocities, and bearings of the three humans engaged in these behaviors in Fig. 6, as measured by FRESHR. Scenarios A – F presented in Table I manifest in these behaviors. These are marked in the three plots of Fig. 6(*b*). We note that the measures correctly track the human move in the shared space.

Observe from Fig. 7 that KDF and HSF report safety values that are much higher than GSI. This is because of the averaging used by these scales that generally lift safety value when few but several humans are safe. For example, as Human 3 approaches the robot, where Humans 1 and 2 stay put, which corresponds to scenario F_1 depicting Human 3 breaching the intimate zone according to proxemics, KDF, HSF, and HSA reduce, but not as much as GSI. The latter's overall safety assessment emphasizes approaching humans over others, per proxemics. In addition to the baseline safety scales, it also includes the remapped zonal allotment from the GSI data. Using Eq. 3, each individual GSI is remapped into proxemic zones (intimate, personal, social, public), yielding an interpretable categorical view of safety that aligns with Hall's framework. This visualization highlights the collective safety captured by the GSI based on human's proximity and motion, emphasizing how the closest or most at-risk individual dominates the overall assessment.

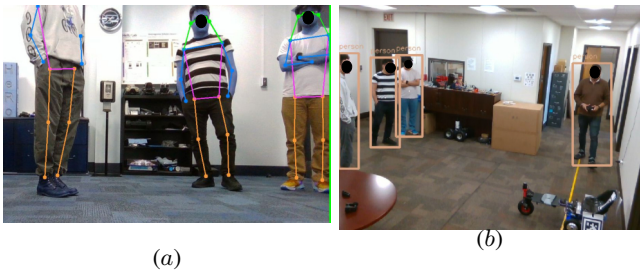

(*a*) (*b*)

Fig. 8: Experimental setup of a mobile robot interacting with multiple humans. (a) Onboard camera perspective shows humans in the robot's immediate vicinity. (b) External viewpoint provides broader context of the shared space and relative positioning. This dual-perspective visualization highlights how dynamic human motion impacts the robot's situational awareness and safety assessment.

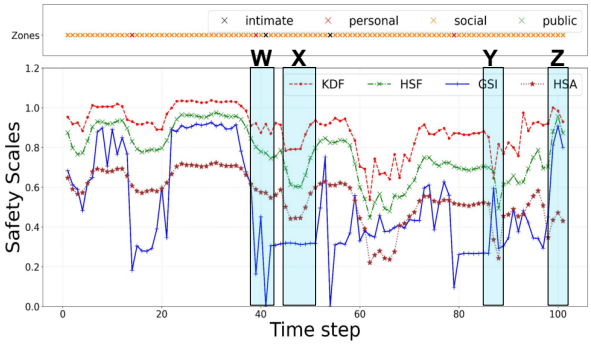

Fig. 9: Output of safety scales from an observer's viewpoint applicable to multiple humans in our experiments with four humans (metrics captured by our FRESHR framework).

A key difference between the safety assessments appears in scenarios D1 and F2. In D1, Humans 1 and 2 move away while Human 3 approaches, so the collective safety should still be dominated by Human 3 as the most at risk individual. In F2, only Human 3 remains within the robot's view, and proxemics indicates the robot is nearing the intimate zone. In both cases, GSI remains sensitive to the approaching human, whereas averaging based baselines are more strongly influenced by the retreating humans, which can lift the overall safety estimate even when one human remains at risk.

In scenario E (Table I), the relative velocity is significantly high (positive), and the robot cannot stop without breaching the human's intimate space, classifying the situation as unsafe. Conversely, in scenario G, if the robot is moving away from the human with high velocity (negative), the scenario is considered safe. Existing safety scales such as KDF and HSA, which assign four times greater weight to distance than velocity, or HSF, which relies solely on distance, tend to misinterpret safety levels in such cases, leading to false assessments. Due to our robot platform's inability to generate high-velocity movements, these two scenarios are not observed in the data.

Based on this detailed analysis, we note that GSI conforms to the proxemics framework, departing from the extant scales such as KDF, HSF, and HSA, even in contexts involving multiple humans. Indeed, KDF and HSF appear to consistently overestimate the overall safety of the situation, whereas GSI offers more specificity in assessing the appropriate safety level of the robot operating in multi-human environments.

Observer's viewpoint: We conducted another experiment in a different setting with an external camera at $\approx 2m$ height overlooking and capturing the movements of four human participants and a dynamic robot's actions. The experiment begins with the robot facing a single person while three others remain stationary at a 90° angle outside the robot's camera view. Additional random movements were introduced to simulate real-world scenarios, requiring the robot to navigate dynamically and avoid collisions with humans.

Although the task robot viewpoint offers a direct safety assessment based on its onboard sensors, it remains inherently constrained by occlusions and a limited field of view (see Fig. 8). In contrast, an external observer viewpoint provides a broader, unobstructed perspective, allowing for a more comprehensive evaluation of multi-human interactions. In simple environments such as narrow corridors without occlusions, the task robot's camera may provide equally effective measurements. Fig. 9 presents the safety scales computed from the observer's perspective, highlighting notable fluctuations in the GSI (blue curve) that are less prominent in the evaluation of the task robot (Fig. 7). These fluctuations primarily arise from dynamic variations in human motion, as all subjects remain within the viewable range of the external camera. In this analysis, factors such as proximity changes, significant velocity changes, and the orientation of all participants are considered. To understand the fluctuations and the difference in the safety scale values, the graph has four regions, W, X, Y, and Z; understanding these regions will provide comprehensive insights into the observed variations.

In region W, initially, GSI drops as human 2 approaches the robot at $1.761m$ with a relative velocity of $1.041m/s$, indicating that the robot may not stop before entering the personal zone. GSI briefly increases at the very next instance, when human 2 stops and human 1 begins moving away, but falls to zero when human 2 accelerates to $1.211m/s$ towards the robot, and as per proxemics, breaching the intimate zone. The rise in GSI occurs when human 2 halts at a safer distance. In the region marked X, the GSI remains stable despite declining other safety scales. This stability results from human 1 maintaining a constant distance of $1.45m$ with negligible velocity, while other humans (positioned $\geqslant 2.4m$) exhibit notable movement. Unlike other scales, GSI prioritizes the closest human, making it more sensitive to immediate risk rather than being skewed by distant movements.

In region Y, GSI initially increases as human 3, who was at the highest risk among others, leaves the view when humans 1 and 2 are at safe distances with low velocities. When human 3 reenters the scene at $1.4m$ with a notable velocity, the stopping distance in proxemics reduces, causing the GSI to drop, capturing the increased risk. In contrast, KDF increases due to reduced velocity influence, while HSF remains stable. Finally, in region Z, all safety scales gradually converge toward higher values as humans move away. HSA lags slightly due to its averaging approach, whereas GSI quickly reflects improved safety by prioritizing the closest at-risk human. This analysis highlights the benefits of an observer-based GSI in multi-human environments, providing a more accurate and responsive safety evaluation than sensors alone.

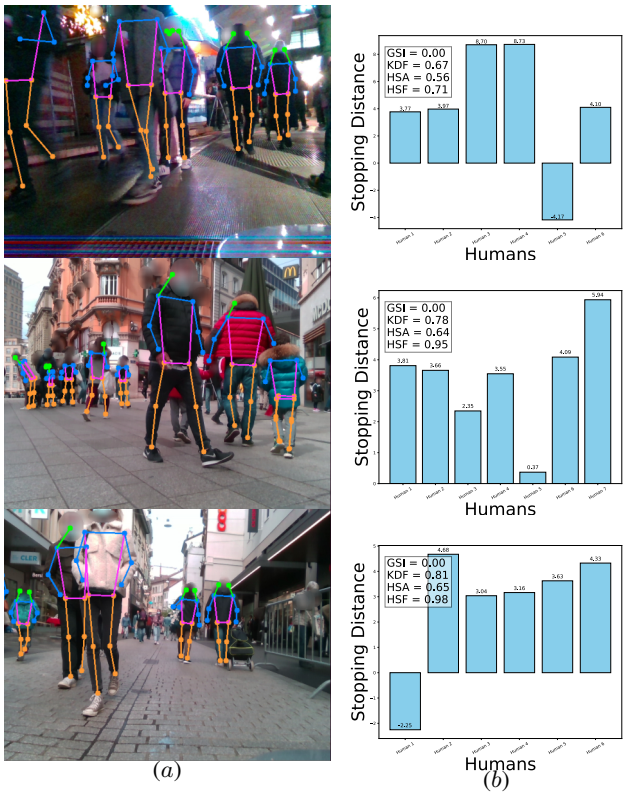

(a) (b)

Fig. 10: Examples from the EPFL Crowdbot dataset illustrating different control modes and corresponding stopping distances of humans used for evaluation. (a) Shows dataset instances for Manual, MDS, and Shared control modes from top to bottom. (b) Shows stopping distances computed from proxemics for the set of tracked humans that pass confidence and visibility filters, which may be fewer than the humans visible in the RGB frame.

C. Evaluating the Utility of GSI in Crowded Environments

We applied our framework to EPFL's Crowdbot datasets [32], which comprise recordings in pedestrian dense street settings with frequent occlusions and varying crowd flow. For each frame, we compute $d_{h,r}$, $v_{h,r}$, and $\theta_{h,r}$ between the robot and each tracked human in the robot's view, and then aggregate via the collective GSI. To avoid bias from unreliable detections in dense crowds, we restrict evaluation to tracked humans that pass confidence and range checks, which can exclude some humans visible in the RGB image. We use GSI to compare control modes that explicitly account for humans versus those that treat humans as static obstacles, comparing autonomous (MDS), manual, and shared control (SC) as shown in Fig. 10(a).Across the three control modes, shared control achieves the highest safety score (0.84 ± 0.37), reflecting that it balances autonomous guidance with timely human intervention in dense interactions. Autonomous MDS achieves 0.80 ± 0.26, typically maintaining efficiency while sometimes accepting closer passes in high flow regions, whereas manual control yields the lowest GSI (0.58 ± 0.32), consistent with the lack of an explicit safety boundary when navigation is driven purely by the operator.

Fig. 10(b) illustrates why other safety scales are unsuitable for accurate safety evaluation. The stopping distance,

determined by the current distance and relative velocity, indicates where the robot will come to a halt. According to proxemics, if this stopping distance is less than 0.46m, the robot is expected to breach the intimate zone, classifying the situation as unsafe. However, other scales reported higher safety values compared to GSI, which failed to reflect the actual risk, demonstrating that GSI provides a more reliable safety assessment by accurately capturing risk levels.

V. Conclusion

This work presents GSI, a proxemics-guided safety assessment model for mobile robot navigation in dense multi-human environments, and FRESHR, an integrated RGB-D vision framework for real-time implementation. Through high-fidelity simulations and physical experiments, we show that GSI yields fine-grained safety metrics and outperforms existing benchmarks in complex social scenarios. These contributions support safety-aware planning, benchmarking, and real-time monitoring in human-rich applications, and motivate future work that combines evaluation signals such as GSI with controllers that provide formal safety guarantees.

References

[1] P. A. Lasota, T. Fong, J. A. Shah *et al.*, "A survey of methods for safe human-robot interaction," *Foundations and Trends® in Robotics*, vol. 5, no. 4, pp. 261–349, 2017.

[2] A. Khalid, P. Kirisci, Z. Ghrairi, J. Pannek, and K.-D. Thoben, "Safety requirements in collaborative human–robot cyber-physical system," in *Dynamics in logistics*. Springer, 2017, pp. 41–51.

[3] M. Valori, A. Scibilia, I. Fassi, J. Saenz, R. Behrens, S. Herbster, C. Bidard, E. Lucet, A. Magisson, L. Schaake *et al.*, "Validating safety in human–robot collaboration: Standards and new perspectives," *Robotics*, vol. 10, no. 2, p. 65, 2021.

[4] J. Palmieri, P. Di Lillo, M. Lippi, S. Chiaverini, and A. Marino, "A control architecture for safe trajectory generation in human–robot collaborative settings," *IEEE Transactions on Automation Science and Engineering*, 2024.

[5] S. Nertinger, R. J. Kirschner, S. Abdolshah, A. Naceri, and S. Haddadin, "Influence of robot motion and human factors on users' perceived safety in hri," in *2023 IEEE International Conference on Advanced Robotics and Its Social Impacts (ARSO)*. IEEE, 2023, pp. 46–52.

[6] F. Ferraguti, M. Bertuletti, C. T. Landi, M. Bonfè, C. Fantuzzi, and C. Secchi, "A control barrier function approach for maximizing performance while fulfilling to iso/ts 15066 regulations," *IEEE Robotics and Automation Letters*, vol. 5, no. 4, pp. 5921–5928, 2020.

[7] D. Kulić and E. Croft, "Pre-collision safety strategies for human-robot interaction," *Autonomous Robots*, vol. 22, no. 2, pp. 149–164, 2007.

[8] M. Lippi and A. Marino, "Safety in human-multi robot collaborative scenarios: a trajectory scaling approach," *IFAC-PapersOnLine*, vol. 51, no. 22, pp. 190–196, 2018.

[9] E. T. Hall, "The hidden dimension," *Garden City*, 1966.

[10] S. Rossi, M. Staffa, L. Bove, R. Capasso, and G. Ercolano, "User's personality and activity influence on hri comfortable distances," in *9th International Conference on Social Robotics: ICSR 2017*. Springer, 2017, pp. 167–177.

[11] H. Kamide, Y. Mae, T. Takubo, K. Ohara, and T. Arai, "Direct comparison of psychological evaluation between virtual and real humanoids: Personal space and subjective impressions," *International Journal of Human-Computer Studies*, vol. 72, no. 5, pp. 451–459, 2014.

[12] B. Leichtmann and V. Nitsch, "How much distance do humans keep toward robots? literature review, meta-analysis, and theoretical considerations on personal space in human-robot interaction," *Journal of environmental Psychology*, vol. 68, p. 101386, 2020.

[13] C. Brandl, A. Mertens, and C. M. Schlick, "Human-robot interaction in assisted personal services: factors influencing distances that humans will accept between themselves and an approaching service robot," *Human Factors and Ergonomics in Manufacturing & Service Industries*, vol. 26, no. 6, pp. 713–727, 2016.

[14] T. Spurný, J. Babjak, Z. Bobovský, and A. Vysocký, "Dynamic proxemic model for human–robot interactions using the golden ratio," *Applied Sciences*, vol. 15, no. 15, 2025.

[15] A. Steinfeld, T. Fong, D. Kaber, M. Lewis, J. Scholtz, A. Schultz, and M. Goodrich, "Common metrics for human-robot interaction," in *Proceedings of the 1st ACM SIGCHI/SIGART conference on Human-robot interaction*, 2006, pp. 33–40.

[16] X.-T. Truong and T. D. Ngo, "Toward socially aware robot navigation in dynamic and crowded environments: A proactive social motion model," *IEEE Transactions on Automation Science and Engineering*, vol. 14, no. 4, pp. 1743–1760, 2017.

[17] R.-J. Halme, M. Lanz, J. Kämäräinen, R. Pieters, J. Latokartano, and A. Hietanen, "Review of vision-based safety systems for human-robot collaboration," *Procedia CIRP*, vol. 72, pp. 111–116, 2018.

[18] I. R. Rodrigues, G. Barbosa, A. Oliveira Filho, C. Cani, M. Dantas, D. H. Sadok, J. Kelner, R. S. Souza, M. V. Marquezini, and S. Lins, "Modeling and assessing an intelligent system for safety in human-robot collaboration using deep and machine learning techniques," *Multimedia Tools and Applications*, vol. 81, no. 2, pp. 2213–2239, 2022.

[19] L. María Amaya-Mejía, N. Duque-Suárez, D. Jaramillo-Ramírez, and C. Martinez, "Vision-based safety system for barrierless human-robot collaboration," *arXiv e-prints*, pp. arXiv–2208, 2022.

[20] P. Svarny, M. Tesar, J. K. Behrens, and M. Hoffmann, "Safe physical hri: Toward a unified treatment of speed and separation monitoring together with power and force limiting," in *2019 IEEE/RSJ International Conference on Intelligent Robots and Systems (IROS)*. IEEE, 2019, pp. 7580–7587.

[21] T. Tashtoush, L. Garcia, G. Landa, F. Amor, A. N. Laborde, D. Oliva, and F. Safar, "Human-robot interaction and collaboration (hri-c) utilizing top-view rgb-d camera system," *International Journal of Advanced Computer Science and Applications*, vol. 12, no. 1, 2021.

[22] S. Secil and M. Ozkan, "Minimum distance calculation using skeletal tracking for safe human-robot interaction," *Robotics and Computer-Integrated Manufacturing*, vol. 73, p. 102253, 2022.

[23] B. Lacevic, P. Rocco, and A. M. Zanchettin, "Safety assessment and control of robotic manipulators using danger field," *IEEE Transactions on Robotics*, vol. 29, no. 5, pp. 1257–1270, 2013.

[24] P. Pandey, R. Parasuraman, and P. Doshi, "Integrating perceptions: A human-centered physical safety model for human-robot interaction," in *2025 34th IEEE International Conference on Robot and Human Interactive Communication (RO-MAN)*, 2025, pp. 1823–1830.

[25] C.-Y. Wang, A. Bochkovskiy, and H.-Y. M. Liao, "Yolov7: Trainable bag-of-freebies sets new state-of-the-art for real-time object detectors," *arXiv preprint arXiv:2207.02696*, 2022.

[26] P. A. Lasota, G. F. Rossano, and J. A. Shah, "Toward safe close-proximity human-robot interaction with standard industrial robots," in *2014 IEEE International Conference on Automation Science and Engineering (CASE)*. IEEE, 2014, pp. 339–344.

[27] A. Edelmann, S. Stümper, and T. Petzoldt, "The interaction between perceived safety and perceived usefulness in automated parking as a result of safety distance," *Applied ergonomics*, vol. 108, 2023.

[28] K. Dautenhahn, M. Walters, S. Woods, K. L. Koay, C. L. Nehaniv, A. Sisbot, R. Alami, and T. Siméon, "How may i serve you? a robot companion approaching a seated person in a helping context," in *Proceedings of the 1st ACM SIGCHI/SIGART conference on Human-robot interaction*, 2006, pp. 172–179.

[29] P. Salvini, D. Paez-Granados, and A. Billard, "Safety concerns emerging from robots navigating in crowded pedestrian areas," *International Journal of Social Robotics*, vol. 14, no. 2, pp. 441–462, 2022.

[30] G. Ferrer, A. Garrell, and A. Sanfeliu, "Robot companion: A social-force based approach with human awareness-navigation in crowded environments," in *2013 IEEE/RSJ International Conference on Intelligent Robots and Systems*. IEEE, 2013, pp. 1688–1694.

[31] T. Jordan, P. Pandey, P. Doshi, R. Parasuraman, and A. Goodie, "Analyzing human perceptions of a medevac robot in a simulated evacuation scenario," in *2025 IEEE/RSJ International Conference on Intelligent Robots and Systems (IROS)*, 2025, pp. 6345–6350.

[32] D. Paez-Granados, Y. He, D. Gonon, D. Jia, B. Leibe, K. Suzuki, and A. Billard, "Pedestrian-robot interactions on autonomous crowd navigation: Reactive control methods and evaluation metrics," in *2022 IEEE/RSJ International Conference on Intelligent Robots and Systems (IROS)*. IEEE, 2022, pp. 149–156.